Effects of Electrode Coverings on Elevated Temperature Properties of Austenitic Stainless Steel Weld Metal

Creep-rupture tests at 1200 F on E308 electrode deposits show a marked dependency on type of electrode

BY N. C. BINKLEY, G. M. GOODWIN AND D. G. HARMAN

ABSTRACT. The creep-rupture properties at 1200 F of deposits made with the flux-covered E308 electrode depend on the type of covering used. Batches of electrodes with lime, lime-titania (approx 25% TiO_2), and titania (approx 50% TiO_2) flux coverings were produced from a single heat of Type 308 stainless steel core wire by a commercial producer. The covering formulas were adjusted to produce weld deposits of essentially identical composition. One-inch thick, Type 304 stainless steel plates were joined with each batch under identical conditions of current, voltage and travel speed. The three different weld deposits exhibited essentially identical deposit composition, ferrite number, and ferrite morphology.

However, the three weldments had significantly different creep-rupture characteristics at 1200 F. The lime-covered electrode deposit exhibited comparatively short rupture times and high ductility. The lime-titania and the titania-covered electrode deposits had significantly longer rupture times at a given stress level, but strained less than 1% before failing at rupture times approaching 1000 h. The lime-covered electrode deposit also demonstrated low fracture ductility at low stresses when tested to rupture.

Introduction

Austenitic stainless steels are candidates for vessels and structural components of advanced high temperature nuclear reactors because of their good high temperature properties and sodium compatability. We are conducting an investigation of high temperature properties of welds and the influence of normal welding and compositional variables on these properties. One such variable is the electrode flux covering used in the manual shielded metal-arc welding (SMAW) process.

Shielded metal-arc electrode coverings are first evaluated on such practical grounds as ease of deposition, bead contour, arc stability, deposition efficiency and ease of slag removal. Satisfactory bend and tensile properties of the weld are also

G. M. GOODWIN is associated with the Metals and Ceramics Div., Oak Ridge National Laboratory, Oak Ridge, Tenn., and N. C. BINKLEY and D. G. HARMON, formerly at Oak Ridge, are now with Babcock & Wilcox Co., Barberton, Ohio and Westinghouse Electric, Tampa Div., Nuclear Energy Systems, Tampe, Fla.

Based on paper presented at the AWS National Fall Meeting, Baltimore, Md., during October 5-8, 1970.

mandatory.[1] The generation of sufficient long-time data in the creep range has not been of major concern in the past because the applications have not required such data. Furthermore, the influence of particlar flux coverings on the creep-rupture properties has received minimal attention. This paper presents creep data for 1200 F tests on Type 308 stainless steel weld metal.

For this investigation, the Type 304 stainless steel base metal and Type 308 stainless steel covered electrode combination was used exclusively.

Currently, the AWS specification[2] (AWS A5.4–69) for stainless steel filler metal recognizes approximately two dozen major classifications of stainless steel covered electrodes, of which Type E308 is only one.[3] The specification requires that an electrode deposit must meet certain chemical analysis requirements in order to comply with any single electrode classification. For electrode diameters of ⅛ to ¼ in., certain tensile test and fillet weld test requirements must also be met. The specification further requires that each classification of electrode type be designated either −15 or −16, depending on the usability characteristics of the electrode. This simply indicates that the conforming batch of electrodes has passed the required tests after being deposited by direct-current, reverse polarity only (−15) or by direct-current, reverse polarity and by alternating current (−16). No requirements are made as to method of manufacture or covering formulation.

However, general classes of stainless steel electrode covering formulas are well known and accepted throughout the welding industry. For example, stainless steel electrodes usually have either a "lime," "lime-titania," or "titania"-type covering. Table 1 gives approximate ingredients one might expect to use in the formulation of the three basic types of stainless steel electrode coverings. Each manufacturer has his own proprietary formulations,[4] but generally the lime-type covering contains more calcium carbonate (limestone) and calcium fluoride (fluorspar) than the titania-type covering and the titania-type covering contains more titanium dioxide (titania). The lime-titania covering is somewhat of a compromise between the other two types.

The lime-type covered electrodes are usually applicable only for direct-current, reverse polarity welding and hence carry the −15 designation.[5] The lime slag which forms during welding is quite viscous and tends to produce a more convex weld bead than the titania-covered electrode deposit. The high viscosity of the lime slag may make the lime-covered electrode more suitable than the titania-covered electrode for welding in the vertical down position.

Table 1 — Typical Covering Compositions for Stainless Steel Electrodes

Covering type	Ingredient, % $CaCO_3$	CaF_2	TIO_2	$NaSiO_4$	$KSiO_4$	Alloy additions and other ingredients
Lime [b]	37	33	3	15		12
Lime-titania	30	15	25	5	10	15
Titania [b]	25	20	35		15	5

(a) Ferromanganese, Ferrosilicon, binders, etc.
(b) Payne et al, Ref. 8.

Table 2 — Deposit Analyses of Experimental Type 308 Stainless Steel Electrodes

Covering type	Composition, % Cr	Ni	Mn	Si	S	P	C	B
Lime	19.94	9.97	1.72	0.46	0.015	0.011	0.044	0.001
Lime-titania	19.80	9.92	1.76	0.47	0.016	0.012	0.044	0.001
Titania	19.98	9.97	1.73	0.46	0.017	0.012	0.044	0.001

The titania-type covered electrode is most frequently qualified for welding with both alternating current and direct-current, reverse polarity. The high proportion of readily ionizable elements such as titanium and potassium helps promote arc stability. The titania-type covering produces a very fluid slag that tends to yield a rather flat or concave deposit profile. While the bead shape produced by this electrode type helps to minimize finish grinding, the fluid slag produced during welding often discourages welding in positions other than flat. If the electrode qualifies for all-position use, it may carry the −16 designation.

The lime-titania-type covered electrode is gaining popularity as a versatile compromise between the lime and the titania-type covered electrodes. In general, the lime-titania-type covered electrode can be used for welding with both alternating current and direct-current, reverse polarity. As a result, this electrode type is normally given the −16 designation. However, an electrode manufacturer may choose not to include such high proportions of the ionizable elements in his formulation of a lime-titania flux covering. In this case, the electrode would qualify for only direct-current, reverse polarity and would be designated −15. In either case, the lime-titania electrode is generally considered applicable for welding in all positions.

Experimental Data

Three experimental 20-lb batches of the lime-, lime-titania and titania-Type E308 stainless steel electrodes were procured from an industrial manufacturer. The covering formulations used were typical of those commercially available today. The electrode deposits conformed to all applicable specifications, including AWS A5.4–69.

To minimize variation of properties due to slight differences in deposit composition, the three different batches of covered electrodes were made from one heat of Type 308 core wire of 5/32 in. diam. The electrodes were stored in moisture-proof containers before welding. Table 2 shows the as-deposited analyses of the three batches of electrodes which are, for all practical purposes, essentially identical. Chemical analyses also included the following elements not shown in Table 2: V, 0.02%; Ti, 0.05%; Cu, 0.05%; N_2, 0.042%; Nb, < 0.05%; Al, < 0.05%; Mo, < 0.076%; Co, < 0.03%. These weight percentages of minor elements were also essentially identical in all three batches.

Experimental Procedure

The three batches of electrodes were deposited in an essentially identical manner. A high speed, low inertia chart recorder was used to record the voltage and amperage of a 300-amp motor-generator machine during welding. The test coupons were 1-in. thick, Type 304 stainless steel machined from a single plate. The joint geometry consisted of a single-U groove with an 80 deg included angle and a ⅛-in. root face and root opening.

The prepared plates were tacked together with a 3/16-in. thick backing strip of Type 304 stainless steel. Extreme care was taken to remove all dirt and grease from the weld joint prior to welding. Electrodes were removed a few at a time from an elec-

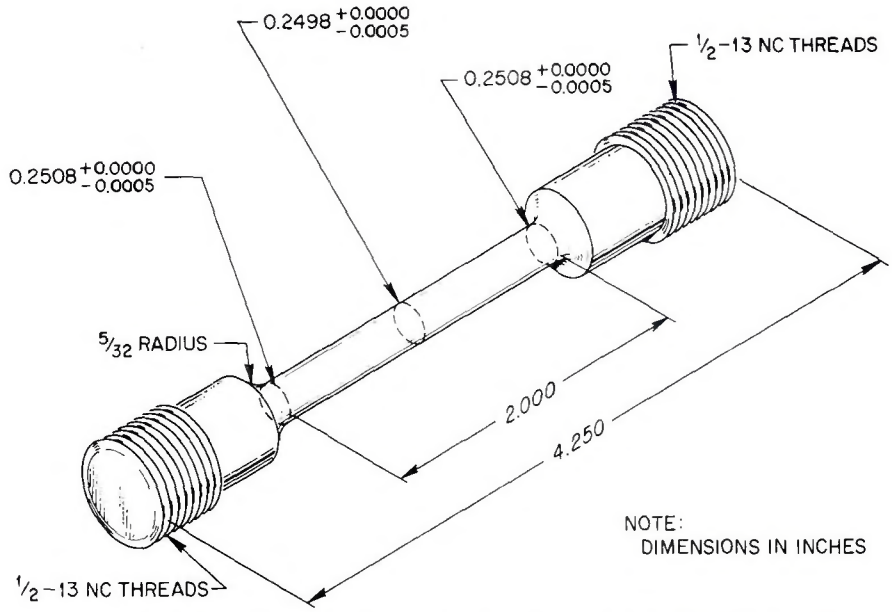

Fig. 1 — Threaded creep-rupture specimen for experimental stainless steel deposits

Table 3 — Deposition Characteristics of Experimental Stainless Steel Electrodes

Covering type	Bead characteristics: Width, in.	Depth, in.	Area in.²	Penetration, in.	Transfer rate drops/sec
Lime	0.403	0.153	0.350	0.0734	2.7
Lime-titania	0.360	0.161	0.344	0.0732	2.7
Titania	0.387	0.160	0.362	0.0718	2.8

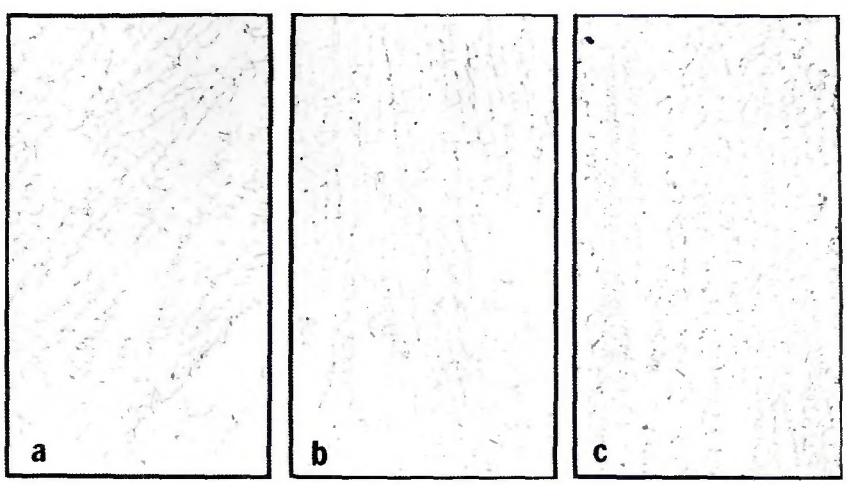

Fig. 2 — Microstructures of weld deposits made by (a) lime covered electrodes, (b) lime-titania-covered electrodes and (c) titania-covered electrodes. Etchant: H_2O, KOH, K_3FeCr_6. Mag. X500, reduced 27%

trode oven to minimize moisture in the covering. Welding was done using qualified procedures and operators and stringer-bead techniques. Slag was thoroughly removed from all passes and all terminal craters were ground out. No preheat was used and interpass temperatures were held below 250 F. The plates were not mechanically restrained during welding.

The chart traces of the three welds facilitated the maintenance of nearly constant welding parameters. Welding was done at an average of 140 amp of direct current, reverse polarity. Arc voltage averaged 26 V, and travel speed was maintained at 10 ipm. These parameters enabled the completion of the weldment in 40–45 passes.

The performance characteristics of each electrode type were evaluated from the chart recordings of a bead-on-plate study. The chart traces of both arc voltage and welding current indicated distinctly the mode of metal transfer across the arc. For example, regular short-circuiting drop transfer is indicated by individual current spikes as the transferring drop of metal bridges the welding arc and creates a short circuit. This is accompanied by a nearly simultaneous decrease of arc voltage. Constant arc voltage and welding current occur with the spray mode of metal transfer. The bead-on-plate study also demonstrated the bead characteristics of an electrode deposit. Four beads of each electrode type were deposited, measured and averaged in terms of bead width, depth, nugget area and penetration below the plate surface.

The completed weldments were 32 in. long and 12 in. wide. The weld faces were about 1½ in. wide. Welds were radiographed prior to specimen removal, and were found to be radiographically sound. Three ¼-in. diam longitudinal, all-weld-metal, stress-rupture specimens (Fig. 1) were machined from each cross section of weld metal, two from the top half and one from the bottom (root) half of the fusion zone.

All creep testing was done in air at 1200 F on the all-weld metal specimens described above. Each weld deposit was tested under these conditions at three different stress levels: 25,000, 20,000, and 18,000 psi. The strain was recorded as a function of time. One specimen of lime-titania weld metal was aged in the unstressed condition at 1200 F for 700 h and subsequently creep tested at 18,000 psi and 1200 F. After testing was completed, failed specimens were examined by optical metallography and scanning electron microscopy techniques.

Results

Table 3 shows the results of the bead-on-plate study. There was little difference in the average bead dimensions; the lime-, lime-titania-, and titania-type covered electrodes all tended to produce deposited beads in the flat position of essentially the same size and shape. This observation is interesting, since the titania-covered electrode is sometimes considered to provide greater penetration than the lime- and lime-titania-type electrodes.

Conventional optical metallography was performed on each deposit type. Figure 2 shows photo-

micrographs at X500 of the three different deposits. There is no obvious difference in the appearance of the three microstructures, and they contain the same nominal amount of ferrite. The amount of ferrite, determined by both Magne-Gage and quantitative television microscope techniques, proved to be about 7-8% by volume. The same amount of ferrite was also predicted by the Schaefler Diagram,[6] based solely on deposit composition.

Also shown in Table 3 are the results of the study to determine transfer rate. It was evident from the chart traces that all three electrode types deposited metal by the short-circuiting drop method. All three pairs of welding current and arc-voltage traces appeared essentially identical. The short-circuit spikes were very regular in all cases and could be easily counted and averaged per unit of time. The results in Table 3 show that the lime-, lime-titania-, and titania-covered electrodes each deposited metal at the rate of 2.7 to 2.8 drops per second of arc time.

Table 4 summarizes the creep-rupture data at 1200 F for specimens tested at three stress levels. The lime-covered electrode weld metal generally had the shortest rupture times and the greatest total elongation at each stress level. The lime-titania- and titania-covered electrode deposits behaved nearly identically, rupturing with low ductility in long-term tests. They strained less than 1% in tests lasting about 600 h. The differences in creep behavior at long times include nearly all of the strain-time characteristics. Figure 3 shows that the minimum creep rate, and the tertiary creep behavior of the lime-covered electrode deposits differ markedly from the titania- and lime-titania covered electrode deposits at the lowest stress. The lime-covered deposit has little "steady-state" or secondary creep strain, while the lime-titania- and titania-covered electrode deposits remain in second-stage creep for relatively long periods of time.

The total elongation is plotted versus rupture time in Fig. 4. The curves indicate that ductility of the lime-titania-covered electrode deposit is slightly lower than that of either the lime-or titania-covered deposits for a given rupture time. The latter two types of deposits have similar ductilities for a given rupture life. However, the ductilities of all three deposits tend toward zero total elongation for rupture times approaching 1000 h.

The results of creep tests on the lime-titania deposit specimens (Fig. 5) show some effect of pretest aging. The aged specimen exhibited only 3% elongation at failure, compared to 10% for the as-welded specimen, and roughly half the rupture life of the unaged specimen.

The fracture surface of the lime-titania-covered electrode deposit that failed after 575 h with only 0.14% total elongation is shown in Fig. 6. The specimen underwent almost no reduction in area. Many cracks occurred along the ferrite-austentite phase boundaries, and they are not limited strictly to the vicinity of the fracture surface. The region on the

Table 4 — Creep-Rupture Test Results on Experimental Covered Electrode Deposits at 1200 F

Covering Type	Rupture time, h			Total elongation, %		
	25,000 psi	20,000 psi	18,000 psi	25,000 psi	20,000 psi	18,000 psi
Lime	27	135	212	22.5	11.5	8.7
Lime-Titania	44	363	575	10.2	3.5	0.14
Titania	26	322	655	23.0	1.1	0.85

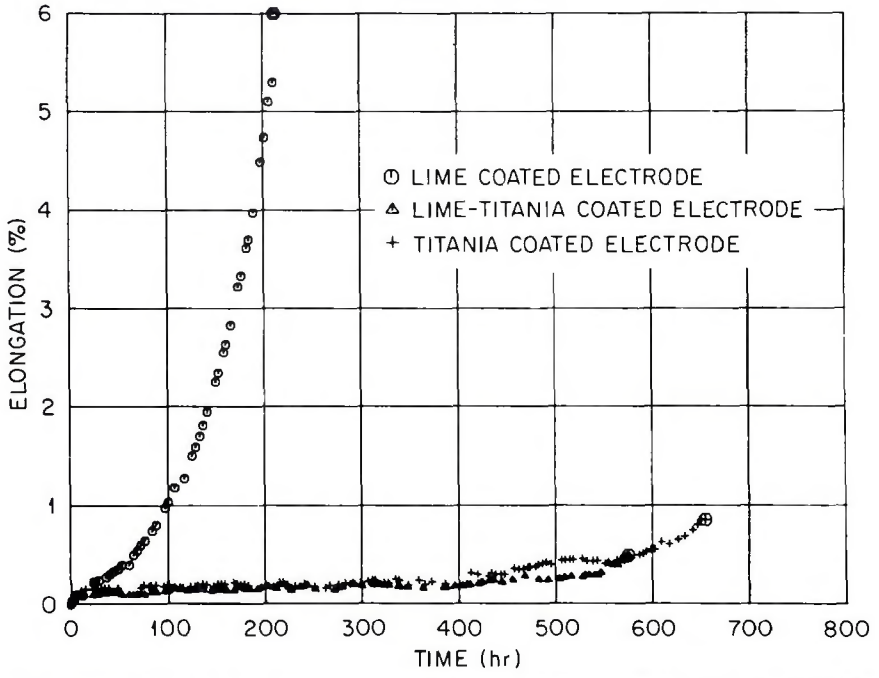

Fig. 3 — Elongation vs time for experimental stainless steel deposits at 1200 F and 18,000 psi

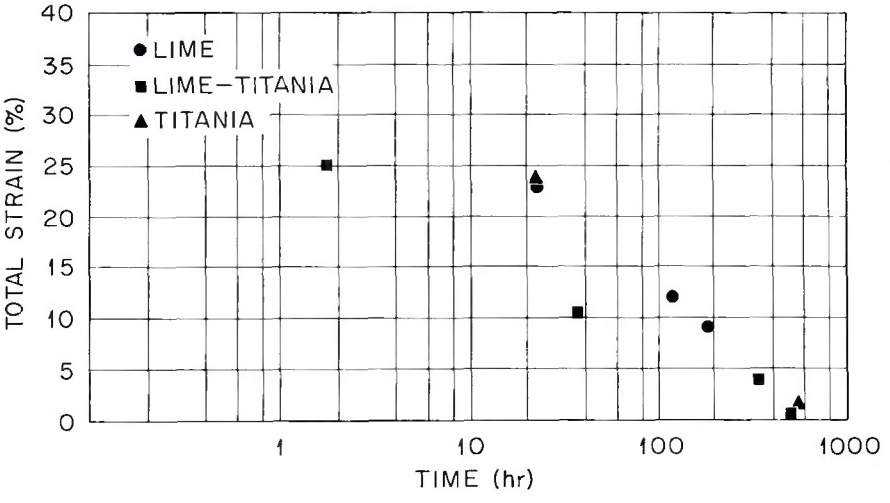

Fig. 4 — Total strain vs time-to-rupture for stainless steel deposits at 1200 F

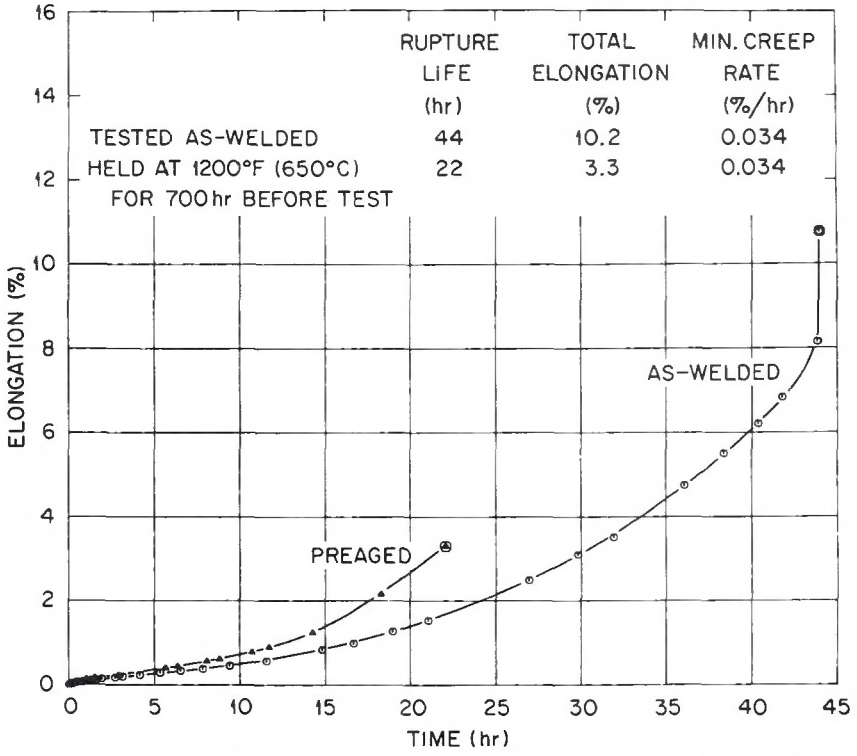

Fig. 5 — Creep curves at 25,000 psi for pretest-aged and as-welded stainless steel weld deposits made with lime-titania-covered electrodes

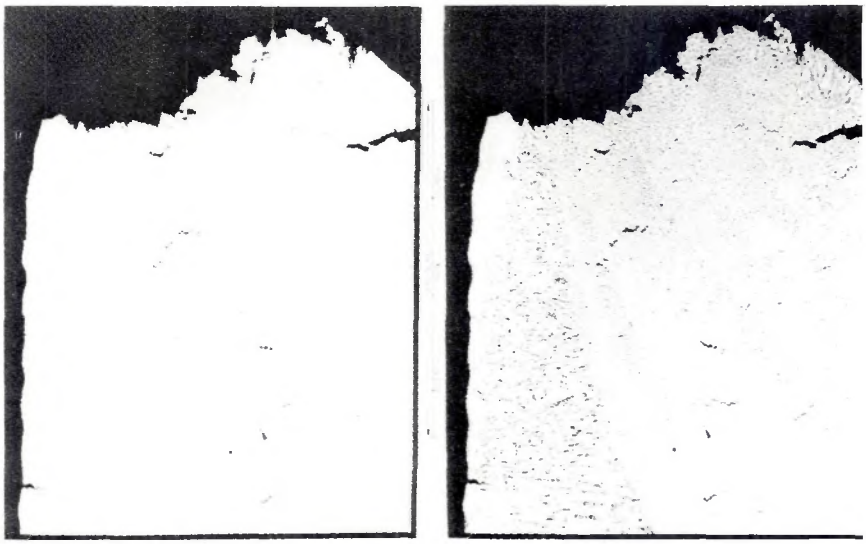

Fig. 6 — Photomicrograghs of fracture of the lime-titania-covered electrode deposit that was creep tested at 1200 F at 18,000 psi stress. Etchant: $K_3Fe(CN)_6$, H_2O. Mag. X100, reduced 20%

left side of Fig. 7 developed fewer cracks under the applied unaxial load than the remainder of the substructure, presumably due to its different substructural orientation.

Scanning electron-microscopy was used to examine the fracture surface of the same specimen. Figure 7 shows four views of the fracture surface at different magnifications. The excellent depth-of-field resolution of the scanning electron microscope permits a very detailed view of the fractured surface. The fracture path has very clearly followed the substructure boundaries.

The optical metallographic examination of the fractured specimen revealed the nature of the time-dependent reaction that apparently causes the severe embrittlement at the interface boundaries. When etched with a warm potassium-hydroxide solution, sigma phase becomes darker than the ferrite constituent. Figure 8 clearly shows the presence of the darkly etched sigma and the lighter etched ferrite in the austenite matrix. The left-hand figure shows that the darker areas are most closely associated with the cracked regions. Since sigma phase in austenitic stainless steel is known to be a hard, brittle constituent,[7] the formation of sigma from ferrite during elevated temperature exposure might be expected to influence the fracture processes in the manner which has been observed here. In related work, sigma was found in large amounts in these weldments after 600 h at 1200 F.

Conclusions

As a result of this investigation, the following conclusions can be drawn.

1. The electrode covering appears to strongly affect the creep-rupture properties of Type 308 stainless steel weld metal.
2. A lime-covered electrode deposit proved to be weaker in creep-rupture testing at 1200 F than either lime-titania- or titania-covered electrode deposits.
3. All three types of covered electrode deposits exhibited decreasing ductility with increasing rupture times in 1200 F creep tests. Ductility as measured by total elongation was less than 1% in a 2-in. gage length for tests of about 600 h and longer.
4. The loss of ductility was associated with time-dependent formation of sigma-phase at the ferrite-austenite substructure boundaries. Sigma phase was identified at the sites where low-ductility fractures initiated.

Acknowledgments

This research was sponsored by the U.S. Atomic Energy Commission under contract with Union Carbide Corporation.

The authors gratefully acknowledge the significant contribution made by Combustion Engineering, Chattanooga Division, especially Messrs. C. T. Ward and E. W. Pickering, Jr., both in preparing the experimental electrodes used in this work, and for corroborating on subsequent work which reduces the ductility problems discussed here. Thanks are also due to C. E. Smith for preparing the test welds, C. W. Walker for assistance in mechanical properties testing, B. C. Leslie for metallographic analysis, and M. R. Hill of the Metals and Ceramics Division Reports Office for preparation of the manuscript.

References

1. "Welding Qualifications," ASME Boiler and Pressure Vessel Code, Sec. IX, The American Society of Mechanical Engineers, New York, 1971.

2. AWS A5.4–69 *Specification for Corrosion-Resisting Chromium and*

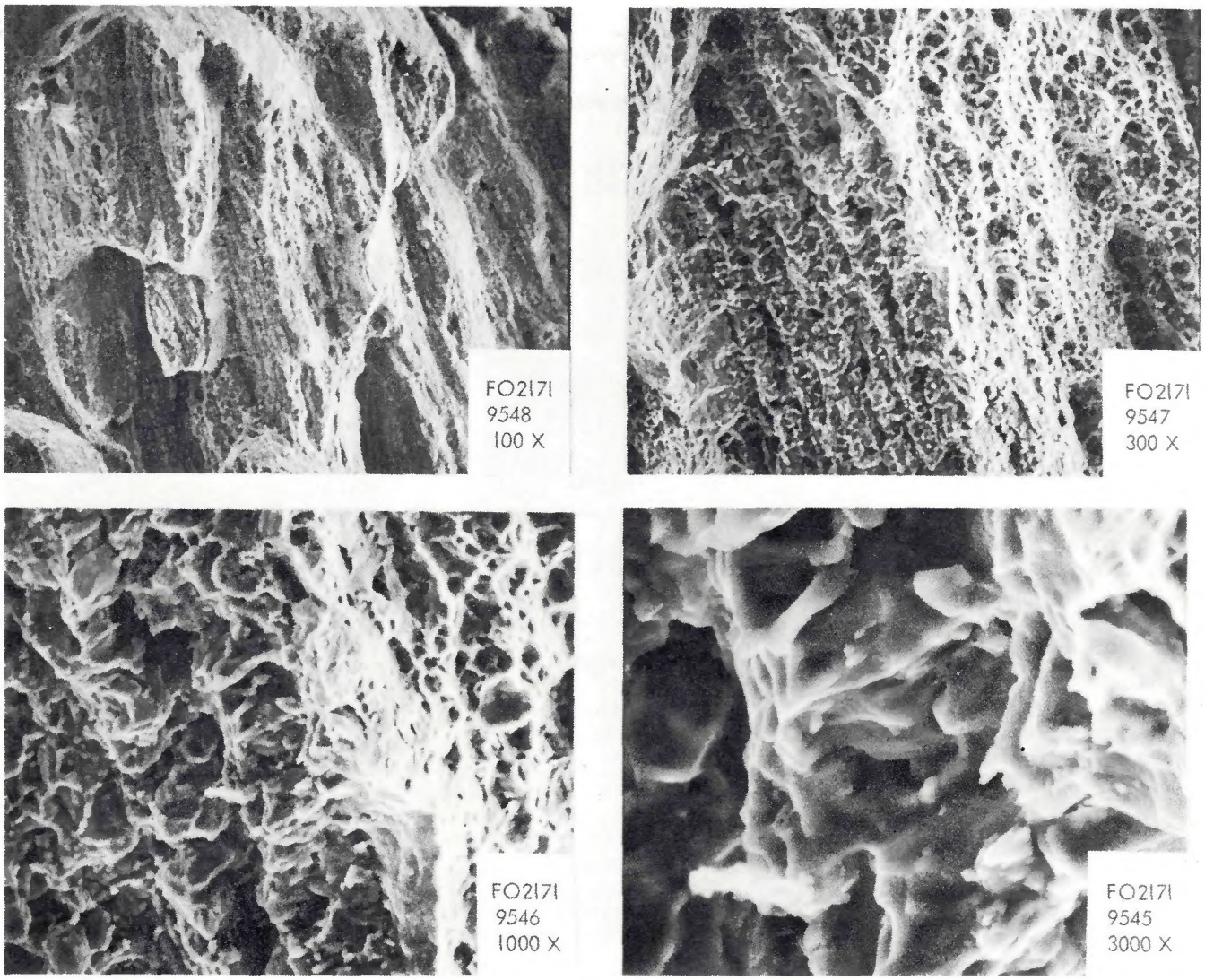

Fig. 7 — Scanning electron micrographs of low ductility weld metal fracture surfaces. Mag. as shown, reduced 18%

Chromium-Nickel Steel Covered Welding Electrodes, American Welding Society, Inc., 1969.

3. "Austenitic Chromium-Nickel Stainless Steel," Section 4, Chap. 65 in *Welding Handbook,* 6th ed., American Welding Society, 1971.

4. Reed, H. F., "It Still Isn't Mud," *Weld. Eng.* 53(1): 45-9 (January 1968).

5. "Filler Metals," Section 5, Chap. 95 in *Welding Handbook,* 5th ed., American Welding Society, 1967.

6. Schaeffler, A. L., "Selection of Austenitic Electrodes for Welding Dissimilar Metals," *Welding Journal,* 26(11), Nov., 1947, Research Suppl., 601-s to 620-s.

7. *Effects of Residual Elements on Properties of Austenitic Stainless Steels, Spec. Tech. Publ. 418,* American Society for Testing and Materials, Philadelphia, 1967.

8. Payne, B. S., Dormer, G. J., and Haslip, L. R., "Lime Coated vs Titania Coated Stainless Steel Electrodes," *Welding Journal,* 41(2), pp 115 to 126, Feb., 1962.

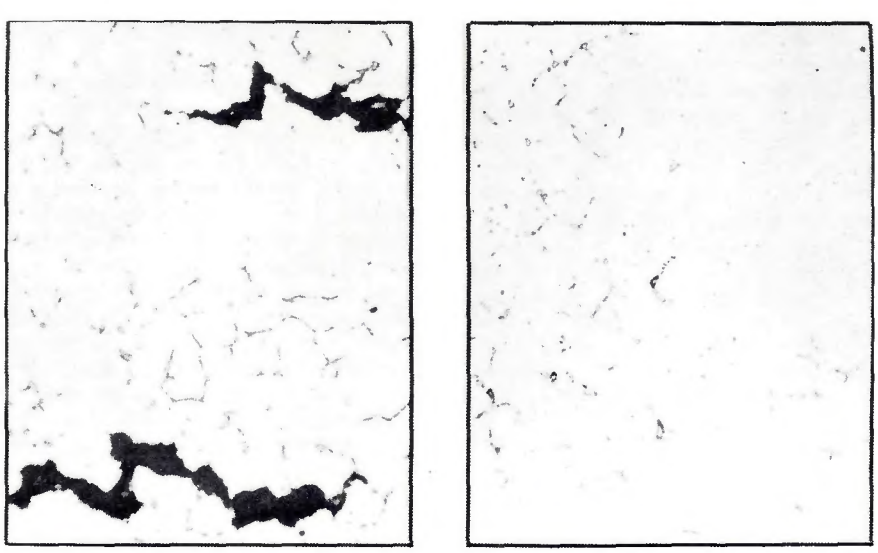

Fig. 8 — Sigma phase (dark-etching constituent) in Type E308 stainless steel deposit fractured after 600 h at 1200 F with less than 1% total elongation. Etchant: 10N KOH. Mag. X750, reduced approx. 41%